JOURNAL OF AGRICULTURAL AND FOOD CHEMISTRY

Phenolic Compounds Contribute to Dark Bran Pigmentation in Hard White Wheat

MARIA A. MATUS-CÁDIZ,*,† TIMOTHY E. DASKALCHUK,‡ BRIJ VERMA,† DEBBIE PUTTICK,‡ RAVINDRA N. CHIBBAR,† GORDON R. GRAY,† CONNIE E. PERRON,† ROBERT T. TYLER,§ AND PIERRE HUCL*,†

Department of Plant Sciences and Crop Development Centre (CDC) and Department of Food and Bioproduct Sciences, University of Saskatchewan, 51 Campus Drive, S7N 5A8 Saskatoon, Saskatchewan, Canada; and Phenomenome Discoveries Inc. (PDI), 204-407 Downey Road, S7N 4L8 Saskatoon, Saskatchewan, Canada

Unacceptably dark bran color has prevented the white-kernelled variety Argent from meeting grain color marketing standards for hard white wheats (*Triticum aestivum* L.). The objective of this research was to identify phenolic compounds that negatively affect bran color in white wheat using Fourier transform ion cyclotron resonance mass spectrometry (FT-ICR-MS) and vanillin−HCl and NaOH staining methods. In mature bran, FT-ICR-MS detected derivatives of the flavonol quercetin in varieties Argent and RL4137 (red-kernelled wheat) but not in W98616, a white wheat variety with acceptable grain color. Derivatives of the isoflavone formononetin were more abundant in W98616 relative to RL4137 and Argent. Vanillin−HCl staining indicated that RL4137 sequestered high levels of proanthocyanidin (PA) throughout its entire seed coat, whereas white wheats sequestered PAs as discrete speckles. Argent possessed abundant speckles over its entire seed coat, whereas speckles were almost undetectable in W98616. In mature kernels, flavonoids throughout the seed coat of RL4137 reacted with NaOH, but only the speckles appeared to react in white wheats. W98616 consistently had lighter grain than Argent before and after NaOH treatment. Free and bound phenolic differences in bran samples confirmed that the darker seed coat color of Argent, relative to W98616, was likely due to higher total phenolic acid content. Although isoflavones accumulated in Argent and RL4137, it appears that the majority of the flux through the flavonoid pathway ultimately accumulates quercetin derivatives and PAs. In W98616, PAs accumulate, but it appears that flavonoid biosynthesis ultimately accumulates isoflavones. Argent, compared to W98616, generally accumulated higher levels of total phenolics (flavonols, stilbenes, and PAs) within its darker pigmented bran.

KEYWORDS: ***Triticum aestivum;*** **FT-ICR-MS; seed coat; vanillin−HCl; phenolic compounds**

INTRODUCTION

In Canada, kernel color has become an important discriminator between hard red-kernelled Canada Western Red Spring (CWRS) and hard white-kernelled Canada Western Hard White Spring (CWHWS) wheat (*Triticum aestivum* L.) classes with the recent introduction of the latter class. Wheat cultivars from both classes have hard grain endosperm for making bread, but their bran colors differ. White-kernelled wheat is preferred for principal foods in Mexico and Asia (*1*). There are several potential reasons for favoring hard white wheat over hard red including higher flour extraction rate, higher flour protein concentration at high flour extraction levels, greater aesthetic appeal of whole wheat products, more valuable bran, better scoring on the basis of flour color standards, and reduced bitter flavor requiring less sugar to make products palatable. The American variety Argent (experimental designation ND690) was the first hard white wheat released by North Dakota in 1998. From a grain marketing standpoint, Argent did not meet USDA Federal Grain Inspection Service (FGIS) color standards as a white wheat, and thus it was classified by the FGIS as a hard red spring wheat. Thus, Argent is genetically white-kernelled but has unacceptably dark grain color from a marketing standpoint for a white-kernelled wheat. Little information exists identifying phenolics that darken the grain color in white-kernelled wheat (*2*).

Over 6000 different flavonoids have been reported and subdivided into different classes that include flavones, flavonols,

* Corresponding authors [(M.A.M.-C.) e-mail maria.matus-cadiz@usask.ca; (P.H.) e-mail pierre.hucl@usask.ca].

† Department of Plant Sciences and CDC, University of Saskatchewan.

‡ Formerly at PDI. Currently, T.E.D. is affiliated with Agriculture and Agri-Food Canada, Saskatoon Research Centre, and D.P. is with the National Research Council of Canada, Plant Biotechnology Institute.

§ Department of Food and Bioproduct Sciences, University of Saskatchewan.

10.1021/jf072970c CCC: $40.75
Published on Web 02/07/2008

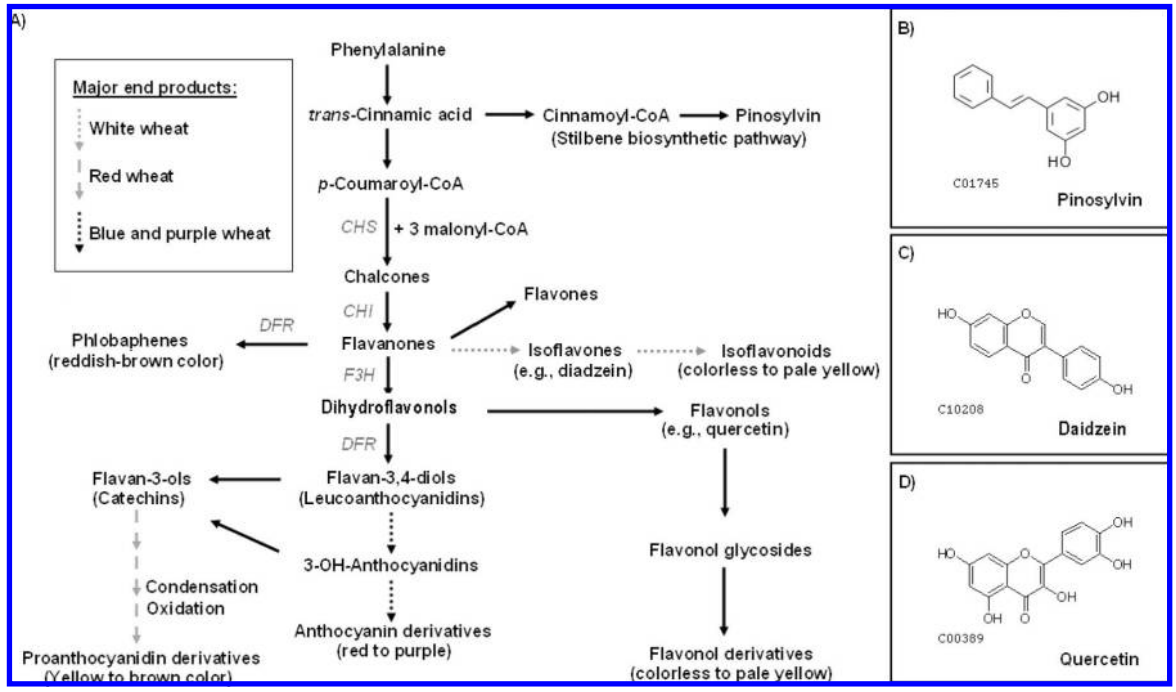

Figure 1. General outline of the flavonoid biosynthesis pathway (adapted from refs *3, 5*, and *27*). (**A**) 4-Coumaroyl-CoA is converted into chalcone by chalcone synthase (CHS), whereas chalcone is converted to flavanone (naringenin) by chalcone isomerase (CHI). Oxidation of naringenin by flavanone 3-hydroxylase (F3H) yields dihydroflavonol. Flavanones are subsequently converted to flavan-3,4-diols by dihydroflavonol reductase (DFR). Derivatives of flavan-3,4-diols can ultimately yield condensed tannins (PAs) and anthocyanins. Dihydroflavonol reductase is also involved in converting naringenin into flavan-4-ols, which are ultimately polymerized to form phlobaphenes. The structures of the stilbene pinosylvin [IUPAC name 5-[(*E*)-2-phenylethenyl]benzene-1,3-diol] (**B**), isoflavone daidzein (7-hydroxy-3-(4-hydroxyphenyl)chromen-4-one) (**C**), and flavonol quercetin (3,3′,4′,5,7-pentahydroxy-2-phenylchromen-4-one) (**D**) are presented. The number beside each molecule is the KEGG database compound identification number. Proposed major end products in the bran of red (*2, 26*), blue (*33*), purple (*33*), and white wheats are indicated.

flavanols, and anthocyanins, according to the oxidation level of the C-ring [(*3*); **Figure 1**]. Stereochemistry, position, and nature of the substitutions (hydroxyl, methyl, galloyl, glycosyl, acetyl), combination, degree of polymerization, and linkages between the basic units allows for the multitude of compounds characterized in plants. The major types of flavonoids in seeds are flavonols, anthocyanins, phlobaphenes, isoflanones, and proanthocyanidins (PAs, also called condensed tannins). The majority of flavonoids exist naturally as glycosides with the addition of hydroxyl groups and sugars increasing their water solubility, whereas other substituents, such as methyl ethers or modified isopentyl units, make flavonoids lipophilic or hydrophobic (*4*). Flavonoids, particularly hydrophobic aglycone forms, are toxic endogenous chemicals for cellular processes because of their high chemical reactivity and thus need to be removed from the cytoplasm immediately after their synthesis (*5*). This removal can occur either by sequestration in the central vacuole (e.g., anthocyanins, PAs, and flavonol glycosides) or by excretion into the cell wall (e.g., polymethylated flavonol glycosides). Vacuoles offer a larger storage space than cell walls, which is important for flavonoids to reach concentrations great enough to function in protection against predators and pathogens or as UV light sunscreens or attractants.

Red grain color in wheat is a highly heritable trait (*6*) and is determined by the *R* genes located on the distal end of the long arms of chromosomes 3A, 3B, and 3D (*7, 8*). Each *R* gene (*R1* on 3D, *R2* on 3A, and *R3* on 3B) was dominant and showed a monogenic inheritance. The three *R* genes controlling seed coat color in hexaploid wheats act in an additive way in that each additional gene results in at least some intensification of the red color (*9*). Researchers have suggested that the *R* genes are transcription factors that regulate flavonoid biosynthesis in wheat (*10*). Studies have suggested that there may be as many as six minor genes influencing grain color in wheat (*11, 12*), in addition to the three major loci controlling red seed color.

The NaOH color test can be used by breeders to quickly differentiate red- from white-kernelled genotypes in wheat (*13*). The NaOH color reaction in red versus white wheats is not well understood. At least one compound in wheat, possibly a flavone, gives a relatively strong yellow color when treated with NaOH. After NaOH treatment of whole grain samples, red-kernelled genotypes (with alleles for red pigment production) turn a brownish orange color, and white-kernelled genotypes (without alleles for red pigmentation) turn a yellow color. In the absence of any interfering color, a white-kernelled wheat kernel placed in NaOH becomes straw yellow in color (*13*). The fact that the brown color is indeed in the seed coat layer is easily demonstrated by slicing open a kernel after color development. Recently, we reported that a diverse set of hard white-kernelled wheats ranged in grain lightness from dark to light after NaOH treatment (*14*). Ranking among genotypes remained constant across environments, suggesting that the gradient in grain lightness was influenced more by genetic than environmental differences. Thus, identifying and ultimately eliminating, through plant breeding, the phenolics darkening the grain color of hard white-kernelled wheat are important from a grain quality and marketing standpoint. The objective of this research was to identify phenolic compounds that negatively affect bran color in white wheat using Fourier transform ion cyclotron resonance mass spectrometry (FT-ICR-MS) and vanillin−HCl and NaOH staining methods.

MATERIALS AND METHODS

Plant Material. In 2004, Argent (white-kernelled genotype; *r1*, *r2*, *r3*), W98616 (white-kernelled; *r1*, *r2*, *r3*), and RL4137 [red-kernelled; *R1*, *R2*, *R3* (*9*)] were grown at the Seed Farm, University of Saskatchewan, Saskatoon, SK, Canada. All genotypes, except Argent, were obtained from the Crop Development Centre, University of Saskatchewan. Argent (Grandin*5/ND614) was obtained from the North Dakota Agricultural Experiment Station, North Dakota State University, Fargo, ND. W98616, a hard white spring germplasm line, was selected from the cross AUS1408/RL4137 (*15*). RL4137 is a red-kernelled germplasm line (*16*). A four-replicate trial was grown using a randomized complete block design. The soil type was a Dark Brown Chernozem clay loam. Individual plots consisted of single rows, 3.6 m long and 0.3 m apart. Plots were sown on June 3, 2004, at a rate of 250 seeds m^{-2} on fallow land. Seeds were treated with the systemic fungicide Vitavax Single Solution (Uniroyal Chemical Ltd., Elmira, ON, Canada; active ingredient carbathiin) at the recommended rate. Fertilizer was drilled in with the seed at a rate of 7 kg ha^{-1} of N and 29 kg ha^{-1} of P. Weeds were controlled with the herbicides Buctril-M (Aventis CropScience Canada Co., Regina, SK, Canada; active ingredients bromoxynil and MCPA) and Puma Super (Aventis CropScience Canada Co., active ingredient fenoxaprop-*p*-ethyl) at recommended rates. Five main, immature spikes at 25 days postanthesis (DPA) were harvested from each plot for *in situ* histochemical vanillin−HCl staining. Five main spikes at physiological maturity were harvested from each plot for *in situ* histochemical NaOH staining. Plots were combine-harvested at maturity and grain samples were dried using forced air driers.

Harvested grain samples were cleaned using a C-XT2 Dockage Tester (Simon-Day Ltd., Winnipeg, MB, Canada) before quality and grain color analysis. A $^9/_{64} \times {}^3/_4$ in. (3.57 × 19.05 mm) rectangular riddle and a $^5/_{64} \times {}^3/_4$ in. (1.98 × 19.05 mm) rectangular sieve were used to remove shriveled and cracked kernels from grain samples. Color measurements were measured with a Hunterlab color difference meter (Color Quest 45/0, Hunter Associates Laboratory, Reston, VA) as *L** values, which designate the lightness of the sample (100 = white and 0 = black). Disposable Petri dishes (60 × 15 mm) were filled to half their capacity with about 10 g of grain. The dishes were covered with their corresponding lids before grain color determinations using the colorimeter. For grain samples treated with NaOH, the grain within each dish was treated with 15 mL of 1.25 M NaOH with 1% Triton X-100 for 1 h at 24 °C on the basis of a previously described method (*13*). Excess NaOH solution was removed from each dish using an aspirator. Dishes were covered with their corresponding lids before grain color determinations. One-way ANOVAs were conducted using Minitab version 13 (Minitab Inc., State College, PA).

For each genotype, a composite grain sample derived using the four field replications was used to obtain bran samples for FT-ICR-MS analysis and phenolic acid determinations. For milling, grain was tempered over an 18 h period to 15.5% moisture. The tempered grain samples were milled on a Quadrumat Jr. flour mill (Brabender Co., South Hackensack, NJ). Milled grain was sifted on a 425 μm mesh sieve (US Std. no. 35; Tyler no. 35) with a Ro-Tap sieve shaker (Tyler Co., Mentor, OH) for 3 min. The material retained on the sieve was considered to be the bran fraction. Bran flakes were ground to pass through a 1 mm screen on a cyclone sample mill (Udy, Fort Collins, CO) to produce ground bran. Approximately 25 g of ground bran of each genotype was obtained by milling 100 g samples. Milled bran samples were stored in sealed plastic bags at −20 °C in darkness and used within 30 days of milling.

FT-ICR-MS and Statistical Analysis. Each bran sample (100 mg) was ground and extracted as three replicates. Bran pigments were extracted as previously described (*17*) by placing 50 mg of bran residue into a 13 × 100 mm glass screw-capped tube and adding 2.5 mL of 1.25 M NaOH. Samples were vortexed, heated at 100 °C for 45 min, and subsequently allowed to cool to room temperature. Approximately 600 μL of 6 N HCl was added to each sample and thoroughly mixed (pH 1.0). Following sample acidification, 1 mL of *n*-butanol was added to each sample, vortexed, and centrifuged at 3000*g* for 10 min at 4 °C. The supernatant (*n*-butanol fraction) was saved and analyzed for pigment content using Phenomenome's proprietary methodology. The supernatants were also analyzed at an absorbance of 495 nm on a Shimadzu DU 800 spectrophotometer (Nakagyoku, Japan) to ensure pigments were extracted from the bran residue (*17*).

Fourier transform ion cyclotron resonance mass spectrometry (APEX III FT-ICR-MS, Bruker Daltonics, Billerica, MA) was used to analyze bran samples for their metabolite content as described previously (*18, 19*). These analyses were conducted by Phenomenome Discoveries Inc. using proprietary methodology (www.phenomenome.com/research/analytics/metabolomics/; verified Jan 2008). The advantage of FT-ICR-MS over other mass spectrometry-based metabolomics methods is its extremely high resolving power ($^1/_{1000}$ of a dalton) and mass accuracy ($^1/_{100000}$ of a dalton). The ultrahigh mass accuracy of the FT-ICR-MS enables assigning of an accurate mass tag to each metabolite detected, which enables the accurate determination of the molecular formula and class of each metabolite detected. Samples were directly injected into the FT-ICR-MS according to the mode of analysis (aqueous or organic) and source of ionization (positive or negative electrospray ionization or atmospheric pressure chemical ionization). All samples analyzed contained internal standards, which were used to calibrate both the mass and intensity for each sample in each run. FT-ICR-MS data files generated for all modes in each sample were manually peak-validated. The resultant data files for all modes of analysis in each sample were formatted to a single DISCOVAmetrics file for each sample analyzed. The metabolome data for the bran samples were displayed independently using *DISCOVA* metrics 2.7 software (Phenomenome Discoveries Inc.). The resulting array was first sorted by mode of analysis, and identical masses within each code were merged when necessary. The merged array was saved and exported to both Microsoft Excel and Genelinker Gold 4.5 (Predictive Patterns) for further analyses.

Global comparison of samples was done in Genelinker. The entire data set of all putative metabolites was filtered for a signal-to-noise (S/N) ratio of 5 or greater in at least one sample. The filtered data were then $\log_2$ normalized, with statistically significant metabolites ($P \leq 0.01$) being determined by the *F*-test function within Genelinker. Unless otherwise stated, both principal component analysis (PCA) and hierarchical clustering analysis (HCA) were performed on the statistically significant metabolites (Genelinker, $P \leq 0.01$) having a S/N ratio of 5 or greater in at least one sample. Hierarchical clustering was performed using the Euclidean distance measurement with complete linkage. All pairwise analyses were performed in Microsoft Excel, where averages and ratios were calculated for each putative metabolite. Statistically significant differences ($P \leq 0.01$) were calculated using Student's *t* test. A two-tailed, type-two *t* test was used when groups of equal sizes were compared, whereas a two-tailed, type three *t* test was used when groups of unequal sizes were compared. Statistically significant metabolites were subsequently filtered, and metabolites that showed at least a 2-fold difference in each pairwise comparison were retained.

Data Mining and Metabolite Identification. Metabolites were putatively identified on the basis of the deduced molecular formula calculated using an independent molecular formula calculator (www.alchemistmatt.com; verified Jan 2008). The deduced molecular formulas were then searched against two public databases (chemfinder.cambridgesoft.com and www.chemnetbase.com; verified Jan 2008) to identify putative compounds. Chemically related metabolites were identified using *DISCOVA* metrics by using all possible chemical transformations provided in the array tools, with the limit of mass variance set at 3 ppm unless otherwise stated.

***In Situ* Histochemical Vanillin and NaOH Staining.** After harvesting, immature spikes (25 DPA) were stored on ice and vanillin−HCl assays were performed within 2 h of harvesting. The seed coat layer with adhering cuticle and cross cells were separated by hand from two immature kernels per spike (mid-region). Observations were repeated over 20 main spikes per genotype (5 spikes per plot × 4 plots). Immature tissue was stained with a freshly prepared solution of 0.13 M vanillin (Sigma Aldrich, Canada) and 6 N HCl (ACS grade) at room temperature for 10 min (*20*). Vanillin turns red upon binding to flavan-3,4-diols (leucoanthocyanidins) and flavan-3-ols (catechins), which are present as monomers or as terminal subunits of proanthocyanidins. Observations and photographs were done on a Nikon Optiphot light

microscope (Nikon Opt. Co., Tokyo, Japan). Immature kernels were also cut in half and stained in the solution described above for 10 min prior to photographing. Observations and photographs were done on a Nikon Optiphot dissecting scope. For wheat bran staining, 90 cm wide Petri dishes were filled to half their capacity with bran, and subsequently each dish was treated with 15 mL of the solution described above for 30 min prior to photographing.

At physiological maturity, five main spikes were harvested from each plot and air-dried at 24 °C for 7 days. Whole kernels were soaked in a freshly prepared solution of 1.25 M NaOH at room temperature for 30 min (*13*). The seed coat layer with adhering cuticle and cross cells were separated by hand from two NaOH soaked kernels per spike. Observations were repeated over 20 main spikes per genotype. After NaOH treatment of whole grain samples, red genotypes turn a brownish orange color and white genotypes turn a yellow color. Observations and photographs were done on a Nikon Optiphot light microscope. For wheat bran staining, 90 cm wide Petri dishes were filled to half their capacity, and subsequently each dish was treated with 15 mL of the solution described above for 30 min prior to photographing.

Extraction of Free and Bound Phenolic Compounds. Free and bound phenolics determinations were performed using a two-step procedure. Free phenolics from the bran of RL4137, Argent, and W98616 were extracted according to a procedure reported previously (*21*). One gram of bran was mixed for 10 min with 80% (v/v) cold ethanol followed by centrifugation at 2500*g* for 10 min. This process was repeated again, and subsequently the supernatants were pooled, rotary evaporated to ≤5 mL, and reconstituted to 10 mL with water. Bound phenolics were extracted as previously described (*22*) with slight modifications: 2 M NaOH (75 mL) was mixed with bran residue (1 g), which previously had free phenolics removed as described above, and the container was purged with nitrogen to minimize the oxidation of phenolic compounds. The mixture was shaken on a rotary shaker at 2000 rpm for 4 h and then acidified to pH 2 with 2 N HCl. Diethyl ether (100 mL) was added to the mixture, the container was inverted several times, and the phases were allowed to separate and further centrifuged at 1000*g* for 10 min. The supernatant was removed and the process repeated once more with 75 mL of ethyl acetate. The supernatants were pooled, evaporated to ≤5 mL, and reconstituted to 10 mL with water. Phenolic concentrations were determined as previously described (*23*). Briefly, evaporated and reconstituted phenolic bran extracts were pipetted into a test tube and oxidized for 5 min with Folin−Ciocalteu reagent (Sigma Aldrich). To neutralize the reaction, a sodium tartrate solution was added, and the samples were placed in a 40 °C water bath for 30 min. The absorbance of the solution was measured at 765 nm, and concentrations of phenolic compounds were determined against external standards of gallic acid (Sigma Aldrich). The phenolic content of the wheat bran was expressed as micrograms of gallic acid equivalent per gram of bran. All of the solvents utilized were of ACS grade (VWR International, Mississauga, ON, Canada). All extractions were performed in triplicate ($n = 3$) using composite samples. Means were tested to be significantly different ($P \leq 0.05$) from each other using paired *t* tests (Minitab version 13).

Red Pigment Absorbance Scans. Red pigments from the bran of RL4137, Argent, and W98616 were extracted as previously described (*17*) with the following modifications: 1 g of bran was defatted (DFF) by consecutively washing, three times each, with 10 mL of hexane, acetone, and diethyl ether; 1 M NaOH (20 mL) was added to the DFF wheat bran and heated for 30 min in a water bath at 100 °C. After cooling, the solution was acidified (pH 3) with HCl, and 10 mL of *n*-butanol was added. The solution was shaken, and the resulting mixture was centrifuged at 3000*g* for 10 min. The upper *n*-butanol layer was removed and evaporated to 1 mL with nitrogen and filtered through 0.2 μm filters prior to further analysis. The *n*-butanol extracts from all samples were scanned for absorbance from 200 to 800 nm on a Shimadzu DU 800 spectrophotometer. All extractions were performed in triplicate ($n = 3$) using composite grain samples.

RESULTS

Nontargeted Metabolite Identification. FT-ICR-MS analysis (*18, 19, 24*) was used to determine candidate metabolites responsible for gross differences in bran pigmentation among RL4137, Argent, and W98616. In the three bran samples, a total of 1491 unique masses were identified using FT-ICR-MS. Both HCA and PCA resolved the three bran samples using 1491 unfiltered (S/N > 1.0) and 560 filtered (S/N ≥ 5.0) putative metabolites (**Figure 2**). Both HCA and PCA grouped RL4137 with Argent. Separation of W98616 from the Argent and RL4137 group occurred along the first principal component (PC1). Two putative phenolic compounds of masses 492.12641 and 536.18912 with deduced molecular formulas of $C_{23}H_{24}O_{12}$ (glycosylated 3′,4′,5-trihydroxy-3,7-dimethoxyflavone) and $C_{26}H_{32}O_{12}$ (double glycosylated pinosylvin), respectively, were identified in the organic mode of analysis (**Table 1**). These metabolites were among the 10 most important PC1 metabolites (absolute values) identified within bran samples (data not shown), suggesting that bran pigmentation contributed to the separation of W98616 from the other two genotypes. RL4137 and Argent separated along PC2, suggesting metabolites other than pigmentation resolved these two nonrelated samples.

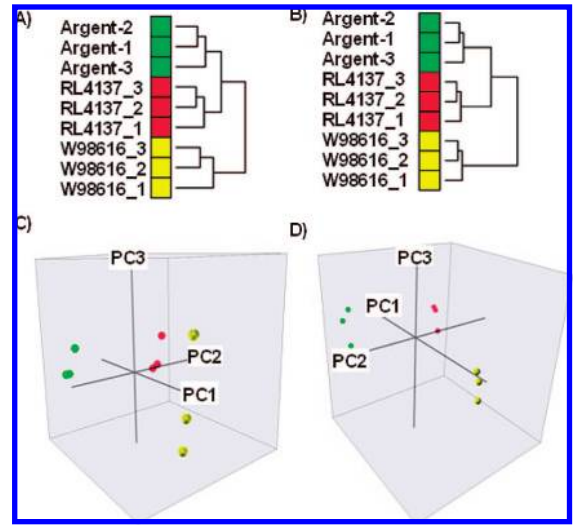

Figure 2. Hierarchical clustering (**A**, **B**) and principal component analysis (**C**, **D**) using 1491 unfiltered (S/N > 1.0) putative metabolites (**A**, **C**) and 560 filtered (S/N ≥ 5.0) putative metabolites (**B**, **D**) identified in bran samples of RL4137, Argent, and W98616.

A pairwise comparison between RL4137 and W98616 identified a total of 484 putative metabolites ($P \leq 0.01$). This list was subsequently filtered for metabolites showing at least a 2-fold difference between the samples, resulting in 85 putative metabolites (36 increased; 49 decreased) in RL4137 relative to W98616 (data not shown). Four groups of metabolites were observed to be either present only in, or at elevated levels in, RL4137 relative to W98616 (>2-fold; $P \leq 0.01$; **Table 1**). A pairwise comparison between W98616 and Argent revealed a total of 432 putative metabolites ($P \leq 0.01$). Selecting metabolites that showed at least a 2-fold difference between the samples resulted in 110 metabolites (31 increased, 79 decreased) in Argent relative to W98616 (data not shown). For the most part, the phenolic-like compounds identified in the RL4137 versus W98616 were also present in the Argent versus W98616 comparison (**Table 1**), suggesting that these metabolites likely contribute, at least in some part, to wheat bran pigmentation.

The first group of metabolites, all derivatives of the flavonol quercetin (**Figure 1**), were in only RL4137 and Argent (**Table 1**). Mass 330.0742 was putatively identified as 3′,4′,5-trihydroxy-3,7-dimethoxyflavone ($C_{17}H_{14}O_7$; **Figure**

Table 1. Four Groups of Metabolites Identified in Bran Samples

putative compd	putative formula	actual mass (Da) theor	actual mass (Da) detected	mass variance (ppm)	mode of analysis	av signal-to-noise ratio[a] W98616	Argent	RL4137
Group 1								
3′,4′,5-trihydroxy-3, 7-dimethoxyflavone	$C_{17}H_{14}O_7$	330.0739494	330.07420	−0.8	organic	0 (0)	2.74 b (3)	4.97 a (3)
glycosylated 3′,4′,5-trihydroxy-3, 7-dimethoxyflavone	$C_{23}H_{24}O_{12}$	492.1267704	492.12670	0.1	organic	0 (0)	5.92 b (3)	8.45 a (3)
3′,4′,5-trihydroxy-3, 7-dimethoxyflavone (glycosylated and acetylated)	$C_{25}H_{26}O_{13}$	534.1373346;	534.13700	0.6	organic	0 (0)	5.92 a (3)	6.27 a (3)
Group 2								
5,7-dihydroxyflavanone; (*S*)-form, 7-*O*-α-L-rhamnopyranoside	$C_{21}H_{22}O_8$	402.1314612	402.13210	−1.6	organic	2.24 b (3)	4.59 a (3)	4.76 a (3)
Group 3								
glycosylated pinosylvin	$C_{20}H_{22}O_7$	374.1365462	374.13670	−0.4	organic	1.88 c (2)	3.89 b (3)	5.30 a (3)
pinosylvin (double glycosylation)	$C_{26}H_{32}O_{12}$	536.1893672	536.18900	0.7	organic	0 (0)	7.66 a (3)	4.72 b (3)
Group 4								
formononetin (glycosylated and methylated)	$C_{23}H_{24}O_9$	444.1420254	444.14130	1.6	organic	8.31 a (3)	3.86 b (3)	1.86 b (3)

[a] Within a row, means for average signal-to-noise ratios ($n = 3$) followed by the same letter are not significantly different at $P \leq 0.05$ using *t* tests. Presented in parentheses are the number of times a metabolite was detected out of three replicated samples within each genotype.

3A), the doubly methylated form of quercetin ($C_{15}H_{10}O_7$). Masses 492.1267 ($C_{23}H_{24}O_{12}$) and 534.137 ($C_{25}H_{26}O_{13}$) appeared to be glycosylated forms of mass 330.0742, with mass 534.137 as the acetylated form of mass 492.1267. The Kyoto Encyclopedia of Genes and Genomes (KEGG) database (www.genome.jp/kegg/; verified January 2008) for flavonoid biosynthetic pathways (www.genome.jp/kegg/pathway/map/map00941.html; verified January 2008) revealed that quercetin is methylated to form 3-methoxyluteolin (3′,4′,5,7-tetrahydroxy-3-methoxyflavone; $C_{16}H_{12}O_7$, mass 316.0583). 3-Methoxyluteolin can be further methylated to form 3′,4′,5-trihydroxy-3,7-dimethoxyflavone ($C_{17}H_{14}O_7$, mass 330.0742), one of the metabolites below detection levels in W98616. Both $C_{17}H_{14}O_7$ and $C_{23}H_{24}O_{12}$ were present at significantly lower levels in Argent compared with RL4137, whereas levels of $C_{25}H_{26}O_{13}$ were similar.

Two other groups of metabolites were observed in W98616 at significantly lower levels relative to RL4137 and Argent (**Table 1**). The metabolite with an accurate mass of 402.13210, 2-fold higher in RL4137 and Argent relative to W98616, was deduced to have molecular formula $C_{21}H_{22}O_8$ and appeared to be the glycosylated form of a dihydroxyflavanone ($C_{15}H_{12}O_3$; mass 240.07864). Masses 374.1367 ($C_{20}H_{22}O_7$; glycosylated pinosylvin) and 536.18900 ($C_{26}H_{32}O_{12}$; double glycocylated pinosylvin) appeared to be the glycosylated forms of the stilbene metabolite pinosylvin ($C_{14}H_{12}O_2$; mass 212.08373) in the stilbene, coumarin, and lignin biosynthetic pathways (**Figure 1**; hultgren.wustl.edu/UTI89/map-nolabel/map00940.html; verified January 2008). Stilbenes (1,2-diarylethenes) belong to a non-flavonoid class of phenolic compounds. Glycosylated pinosylvin was 2−3-fold less abundant in W98616 than in RL4137 and Argent, respectively, whereas double glycosylated pinosylvin levels were below detection in W98616 but almost 2-fold higher in Argent than RL4137 (**Table 1**).

For the fourth group of metabolites, mass 444.1430 ($C_{23}H_{24}O_9$; glycosylated and methylated formononetin), likely an isoflavone (www.genome.ad.jp/kegg/pathway/map/map00943.html; verified January 2008), was the only metabolite found to be significantly more abundant in W98616 compared to RL4137 and Argent (**Table 1**). The metabolite daidzein ($C_{15}H_{10}O_4$; mass 254.05791) is likely methylated to form formononetin ($C_{16}H_{12}O_4$; mass 268.07356), which is subsequently glycosylated and then methylated to yield metabolite $C_{23}H_{24}O_9$ (mass 444.1430, **Figure 3B**).

Hunterlab Color Difference. Wheat genotypes differed significantly in grain lightness (L^* values) before and after NaOH treatment. Before NaOH treatment, RL4137, the only red-kernelled entry, was darker ($L^* = 39.9$; $LSD_{0.05} = 1.0$) than both white-kernelled wheats (Argent, $L^* = 42.8$; W98616, $L^* = 43.9$). NaOH treatment enhanced the differences between red-kernelled RL4137 ($L^* = 24.6$; $LSD_{0.05} = 1.3$) and the white-kernelled genotypes (Argent, $L^* = 35.3$; W98616, $L^* = 37.5$). Whole grain samples of W98616 were lighter than Argent before (L^* difference = 1.1) and after (L^* difference = 2.2) NaOH treatment, with NaOH treatment enhancing their lightness differences.

Sodium Hydroxide and Vanillin Staining. Staining of mature bran (**Figure 4**), whole immature kernels at 25 DPA (**Figure 5A**,**B**), and seed coat layers (**Figures 5C** and **6**) are presented. The NaOH color test quickly differentiated between the red bran of RL4137 and the white bran of W98616 (**Figure 4A**). After NaOH treatment, the red bran of RL4137 turned a brownish orange color, whereas the white bran of W98616 turned a yellow color. In mature bran, the vanillin−HCl color test quickly differentiated between the red bran of RL4137 and the white bran of W98616 (**Figure 4C**). After vanillin−HCl treatment, the red bran of RL4137 turned red, whereas the white bran of W98616 remained colorless, with the red color indicating that vanillin was binding to flavan-3,4-diols (leucoanthocyanidins) and flavan-3-ols (catechins), likely primarily in their condensed and oxidized polymeric forms (PAs). In immature kernels (25 DPA), the vanillin−HCl color test quickly differentiated red-kernelled RL4137 and white-kernelled W98616 (**Figure 5A**,**B**). After vanillin−HCl treatment, the seed coat of RL4137 turned red over its entire seed coat layer, with the

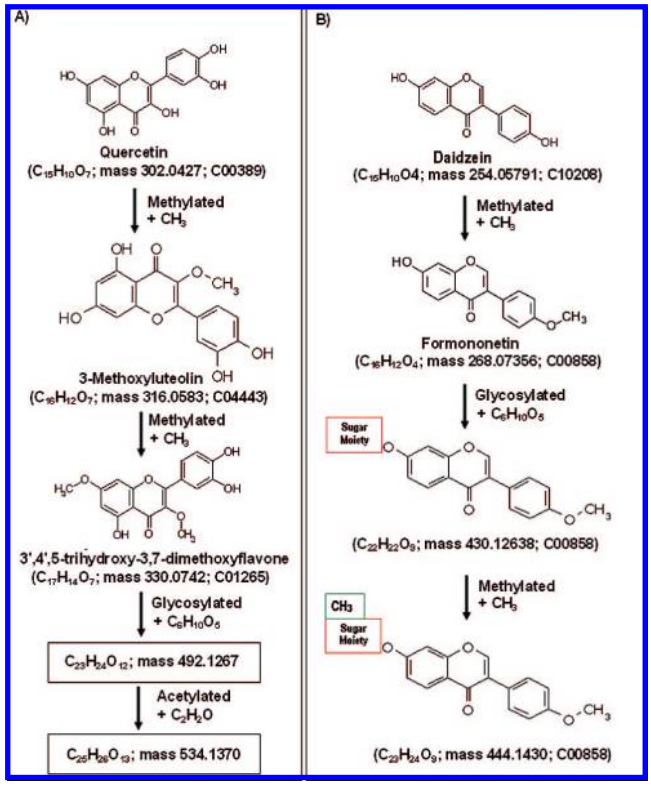

Figure 3. Proposed biosynthetic steps in the formation of derivatives of the flavonol quercetin (**A**) and isoflavone formononetin (**B**). (**A**) Quercetin ($C_{15}H_{10}O_7$; mass 302.04265; C00389) is methylated to form 3-methoxyluteolin ($C_{16}H_{12}O_7$; mass 316.0583; C04443), which is subsequently methylated to form 3′,4′,5-trihydroxy-3,7-dimethoxyflavone ($C_{17}H_{14}O_7$; mass 330.0742; C01265). 3′,4′,5-Trihydroxy-3,7-dimethoxyflavone is glycosylated and then acetylated to produce $C_{23}H_{24}O_{12}$ and $C_{25}H_{26}O_{13}$, respectively. (**B**) Daidzein ($C_{15}H_{10}O_4$; mass 254.05791; C10208) converts to formononetin ($C_{16}H_{12}O_4$; mass 268.07356; C00858), which is glycosylated ($C_{22}H_{22}O_9$; mass 430.12638; C00858) and subsequently methylated ($C_{23}H_{24}O_9$; mass 444.1430; C00858).

red color indicating that vanillin was likely binding to flavan-3,4-diols (leucoanthocyanidins) and flavan-3-ols (catechins), likely in their monomeric forms (**Figures 5C** and **6**). After *in situ* histochemical vanillin−HCl staining, the seed coat of RL4137 turned red over its entire seed coat layer (**Figure 6B**), whereas the seed coats of Argent and W98616 remained colorless except for discrete speckles, which tended to occur more frequently across the seed coat surface of Argent (**Figure 6D**). After *in situ* histochemical NaOH staining, the seed coat of RL4137 turned brown over its entire seed coat layer (**Figure 6A**), whereas generally only the speckles within the seed coats of Argent and W98616 reacted with NaOH (**Figure 6C**,**E**).

Free and Bound Phenolic Compounds. Free and bound phenolic concentrations in the bran of all three genotypes were determined using the Folin−Ciocalteu method. External standards of gallic acid were used for quantification, which gave a linear calibration ($r^2 = 0.99$). The concentration of free phenolic compounds, in gallic acid equivalents, was significantly lower in W98616 compared to RL4137 and Argent (**Figure 7**). Bound phenolic concentrations were lower in W98616 and Argent relative to RL4137. The general trend for total phenolics was one of decreasing phenolic content as the number of *R* genes decreased.

Pigment Absorbance Scans. Seed coat pigments were successfully extracted using alkaline digestion followed by

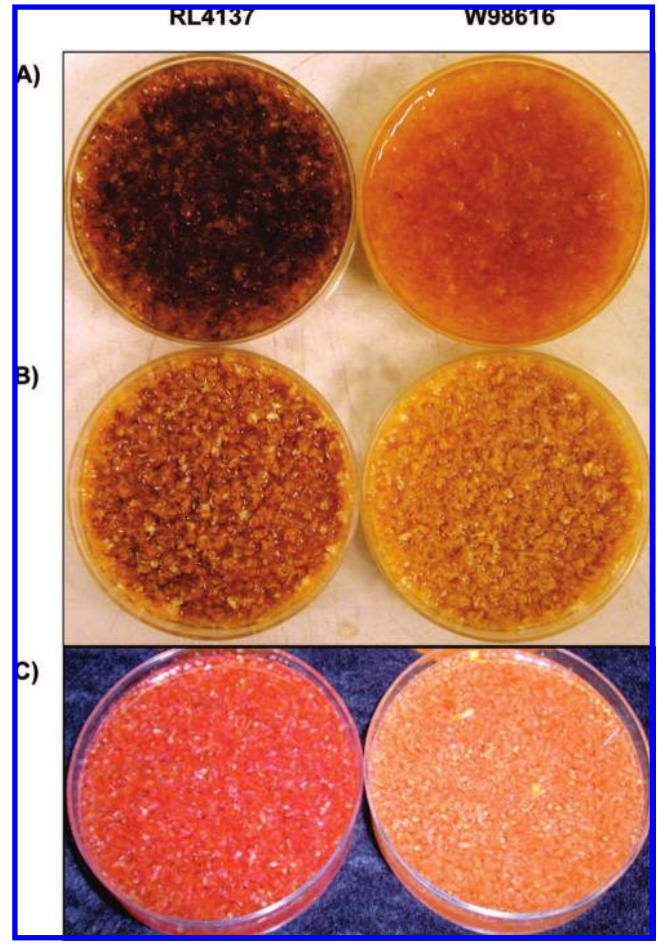

Figure 4. RL4137 and W98616 bran treated with 1.25 M NaOH (**A**), water (**B**), and 0.13 M vanillin−HCl (**C**).

n-butanol extraction (**Figure 8**). The absorbance spectrum of the *n*-butanol-extracted pigments showed that with a decreased number of *R* genes in the wheat cultivars there was a corresponding decrease in the absorbance of the extracts. Absorbance spectra for the extracts of Argent were midway between RL4137 and W98616.

DISCUSSION

In wheat, pigmentation is localized in a seed coat layer, composed of two thin, highly compressed cell layers oriented at right angles relative to each other (*25*). In wheat, the seed coat layer and pericarp are physically united, with the innermost tissues of the pericarp adhering firmly to the cuticle on the outer surface of the seed coat. The cuticle adheres to the cross cells where gaps between the tube cells occur. Mechanical separation of the seed coat into its component parts is extremely difficult. Research has observed a positive relationship between catechin tannin content and degree of seed coat color in immature kernels, with red, light red, and white varieties showing the highest to lowest levels, respectively, of these precursors of brown pigment (*2*). These researchers also reported that the pigment occurs mostly in the seed coat rather than in the pericarp.

Current literature suggests that PAs are derived from catechin tannin (*3*), indicating that white, compared to red-kernelled, wheats accumulate lower levels of PAs within their seed coats (*2*). In *Arabidopsis*, these polymers progressively become colored through oxidative browning (*20*). Researchers

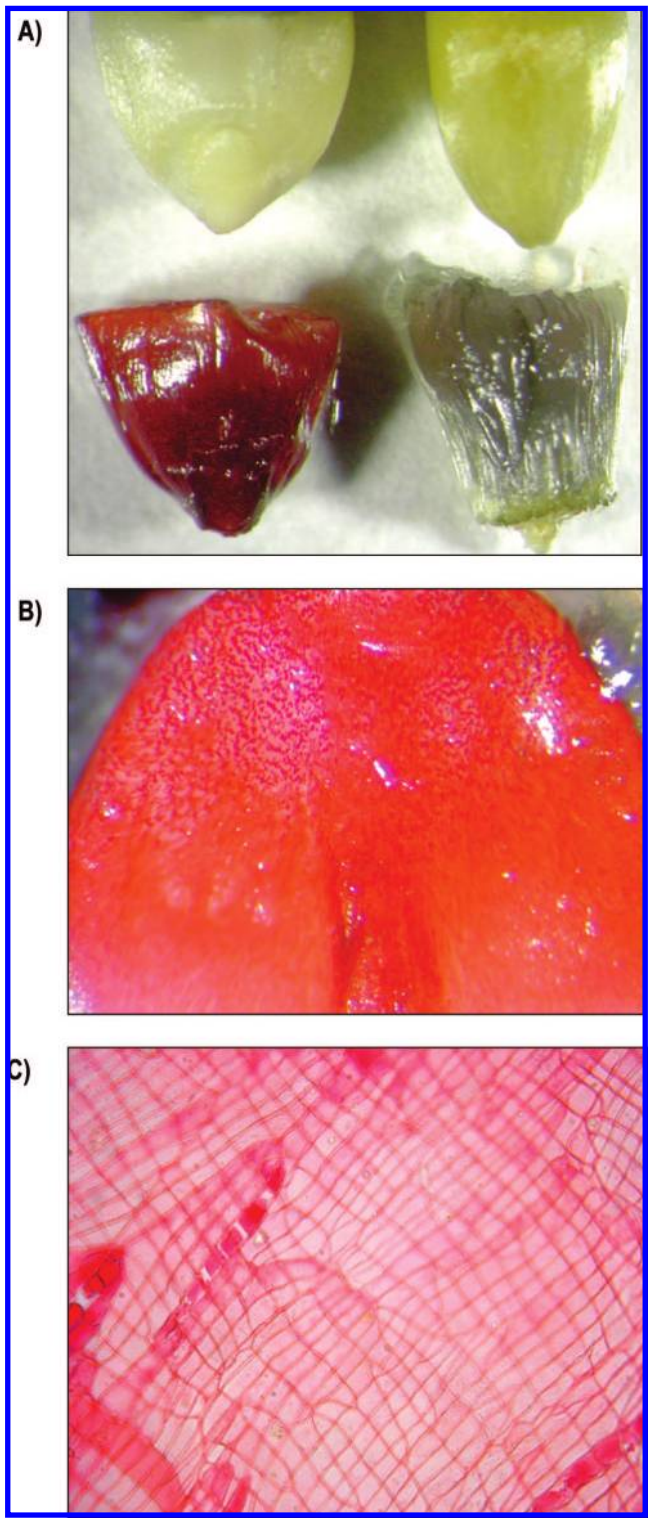

Figure 5. Immature wheat kernels at 25 DPA treated with 0.13 M vanillin−HCl: (**A**) top left and clockwise = RL4137 untreated, W98616 untreated, W98616 treated, RL4137 treated; (**B**) RL4137 kernel; (**C**) RL4137 seed coat (30 DPA) showing two highly compressed cell layers oriented at right angles relative to each other.

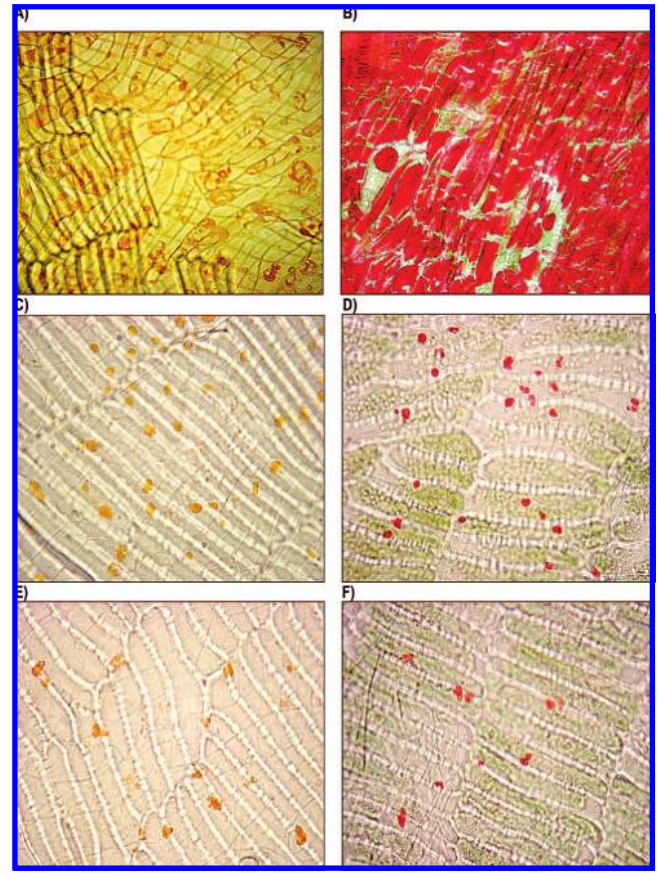

Figure 6. Seed coat layer of wheat kernels treated with 1.25 M NaOH (mature kernels) and 0.13 M vanillin−HCl (immature kernels at 25 DPA) at 40× magnification. NaOH treated: (**A**) RL4137 red-kernelled; (**C**) Argent white-kernelled; (**E**) W98616 white-kernelled. Vanillin treated: (**B**) RL4137; (**D**) Argent; (**F**) W98616. (**E**, **F**) Areas within the seed coat layer where speckles were actually present. The rectangular cross cells in the background have been partially removed in (**A**) to expose the cuticle adhering to the two cell layers in the seed coat.

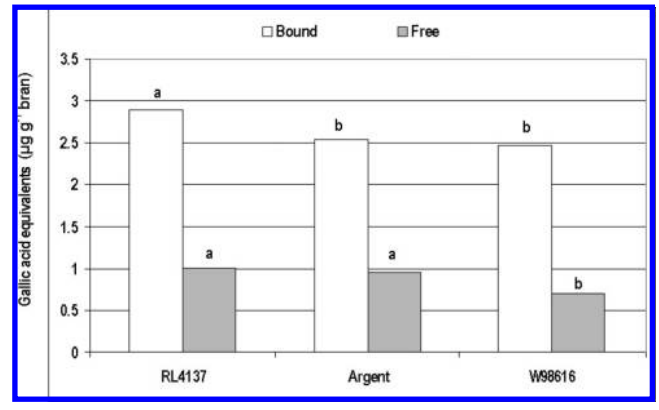

Figure 7. Concentration of bound and free phenolics in RL4137, Argent, and W98616. Within each phenolic group, bars topped by the same letter are not significantly different at $P = 0.05$ on the basis of t tests.

have identified low levels of catechin and di-, tri-, and oligomeric PAs (mostly prodelphinidin with some procyanidin and propelargonidin) soluble in acetone in mature, red-kernelled wheat bran (*26*). However, the amounts of extractable PAs in mature wheat grain appeared to be significantly less than those reported in barley (*Hordeum vulgare* L.). These researchers suggested that the extraction of PAs would likely improve when using immature kernels as enzymatic oxidation and polymerization (*27*) are favored by the breakdown of cellular structure that occurs in the seed coat during grain maturation. Futhermore, researchers have suggested that current estimates of the amount of PAs in seeds are probably too low because during seed maturation PA may interact with other phenolics, proteins, or cell wall polysaccharides to limit their extraction efficiency (*3*). Similarly, it

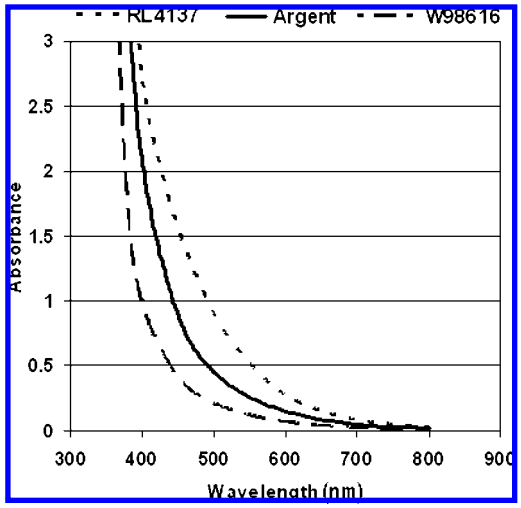

Figure 8. Absorbance spectra of *n*-butanol-extracted bran pigments from RL4137, Argent, and W98616.

has been recommended that analysis of PA at peak deposition in the developing seed coat, rather than in the mature, dehydrated seed, where PA is nearly unextractable, could enable researchers to better quantify PA in yellow- and brown-seeded Brassicaceae germplasm (*28*). In summary, as previously suggested (*3*), improved techniques for extraction, quantification, and characterization of seed and kernel PAs are needed.

Nontargeted FT-ICR-MS analysis differentiated among bran samples of RL4137, Argent, and W98616 by detecting four metabolite groups: (1) derivatives of the flavonol quercetin (flavonol class), (2) a dihydroxyflavanone (a dihydroflavonol), (3) pinosylvin (stilbene, a nonflavonoid phenolic compound), and (4) formononetin (flavone class). The flavonoids existed as glycosides with the addition of hydroxyl groups and sugars, which likely increased their water solubility (*4*), whereas subsequent methylations and/or acetylations likely decreased their water solubility. The flavonoids detected in the bran were present throughout the entire seed coat of RL4137 and only in discrete speckles within the seed coats of white wheats. Similar research has observed that, as a rule, yellow-seeded *Brassica* germplasm had very little PA compared with dark-seeded germplasm, and dark seeds accumulated PA over the entire seed coat (*28*). Furthermore, variation in the concentration of extractable PA from whole seeds of *Brassica napus* was observed among yellow-seeded lines. Vanillin- and NaOH-treated bran, whole kernels, and seed coats indicated that RL4137 followed by Argent and then W98616 possessed a decreasing amount of accumulated phenolic compounds within their respective bran layers. However, the exact mixture of phenolic compounds reacting with the vanillin−HCl and NaOH solutions remains unclear. As in Brassicaceae (*28*), the number of genes controlling seed coat color and pigment accumulation among white wheats has yet to be elucidated. Phenolic acid determinations and red pigment absorbance scans indicated that the darker seed coat color of Argent was likely due to a higher total phenolic acid content. The higher free phenolics in the bran of Argent may explain, at least in part, why this genetically white-kernelled wheat is considered to possess unacceptable grain color for a white wheat. Similar levels of $C_{25}H_{26}O_{13}$ were detected in RL4137 and Argent even though its precursors, $C_{17}H_{14}O_7$ and $C_{23}H_{24}O_{12}$, were present at significantly higher levels in RL4137. This difference is likely explained by poor extraction of glycosylated and acetylated 3′,4′,5-trihydroxy-3,7-dimethoxyflavone from the red bran of RL4137. The amount of free and bound phenolics in mature wheat bran may likely improve using immature kernels, and thus further research is needed.

Recently, researchers reported that four enzymes [chalcone synthase (CHS); chalcone isomerase (CHI); flavanone 3-hydroxylase (F3H); and dihydroflavonol reductase (DFR); **Figure 1**) in the flavonoid biosynthesis pathway were down-regulated in the immature grain of white-kernelled lines, but highly up-regulated in red-kernelled lines (*29*). Myb-type and bHLH-type transcription factors, known to function as key factors for the up-regulation of flavonoid synthesis genes, may play a role in activating the flavonoid biosynthesis genes in the seed coat tissue of red-kernelled wheat (*10*). In wheat, three Myb binding elements were found within the *DFR* promoter, and Myb-type factors were suggested to play an important role in the up-regulation of *DFR* in immature red-kernelled wheat (*30*).

Phenylalanine metabolism feeds directly into the stilbene biosynthetic pathway and indirectly into the flavonoid biosynthetic pathways through *trans*-cinnamate and *trans*-4-hydroxycinnimate with *trans*-cinnamate as a branching point for either flavonoid or pinosylvin biosynthesis (**Figure 1**). Generally, our results are in agreement with current literature (*29*). That is, although some glycosylated and acetylated formononetin accumulated in the red bran (RL4137), it appears that the majority of the flux through the flavonoid biosynthetic pathway is from 4-coumaroyl-CoA to naringenin chalcone and, ultimately, to quercetin derivatives and PAs. In addition, the majority of *trans*-cinnamate is utilized for flavonoid biosynthesis, whereas only a small proportion of *trans*-cinnamate forms glycosylated derivatives of formononetin and pinosylvin. White-kernelled Argent, compared with RL4137, appears to convert a similar proportion of *trans*-cinnamate into formononetin derivatives and a greater proportion into pinosylvin derivatives, particularly the double glycosylated form. In contrast, although PAs accumulate in the white bran of W98616, greater amounts of *trans*-cinnamate are converted into glycosylated derivatives of formononetin, thus favoring isoflavonoid biosynthesis through isoliquiritigenin when producing phenolic compounds. W98616 appears to convert very little *trans*-cinnamate into glycosylated derivatives of pinosylvin and thus, unlike Argent, it does not appear to favor stilbene biosynthesis when producing phenolic compounds within its bran layer. Argent, compared to W98616, generally accumulated higher levels of total phenolics (flavonols, stilbenes, and PAs) within its darker pigmented bran. Further research is needed to elucidate if the elevated levels of isoflavone in W98616 result from a genetic block in the flavonoid biosynthetic pathway that prevents the biosynthesis of 3′,4′,5-trihydroxy-3,7-dimethoxyflavone and its derivatives. Our nontargeted methods suggested that the flavonoid biosynthesis flux in white wheats differs from red wheats and, if confirmed using molecular techniques, could contribute toward a broader understanding of bran pigmentation in white wheat. Further research is needed to (1) identify and characterize the types of transcription factors (*31*) that control flavonol accumulation in different parts of the wheat plant and (2) characterize flavonoid mutants in wheat kernels (*3, 20, 32*).

NaOH treatment enhanced whole grain color differences among the genotypes, with W98616 consistently having lighter grain than Argent before and after NaOH treatment. Recently, we reported that a set of 64 hard white-kernelled wheats, including 60 Australian, 3 Canadian, and the American variety Argent, ranged in whole grain lightness from dark to light after NaOH treatment [$L^* = 31.7-37.4$,

$LSD_{0.05}$ = 1.5; (*14*)]. Argent, one of the white wheats with the darkest grain lightness after NaOH treatment (L^* = 32.5), was not significantly different in grain color from 13 varieties (1 Canadian and 12 Australian), indicating that the L^* value paired with NaOH staining of whole kernels can be used to quickly select for light grain color among white wheats being considered for use as parents within a breeding program. The high frequency of Australian white wheat varieties with light grain color indicates that decades of breeding have resulted in an abundance of varieties with acceptable grain color from a marketing standpoint. Our current research results suggest that higher L^* values appear to indirectly indicate lower total bran phenolics. Thus, we suggest that the NaOH color test paired with a color difference meter could be used to effectively select for lower total bran phenolics among hard white wheat breeding lines. Further research is needed to determine if vanillin−HCl staining paired with a color difference meter could be used to select for lower PA accumulation among hard white wheats by selecting for lower a^* values (designates redness when positive or greenness when negative). The highly corrosive nature of 6 N HCl will likely limit the use of this method.

ABBREVIATIONS USED

Argent, white-kernelled wheat with unacceptable grain color; DPA, days postanthesis; PC1, first principal component; FT-ICR-MS, Fourier transform ion cyclotron resonance mass spectrometry; HCA, hierarchical clustering analysis; KEGG, Kyoto Encyclopedia of Genes and Genomes; PCA, principal component analysis; PA, proanthocyanidin; RL4137, red-kernelled wheat; W98616, white-kernelled wheat with acceptable grain color.

ACKNOWLEDGMENT

Appreciation is expressed to our technical staff for assistance in conducting field studies (K. Jackle; M. Grieman), performing phenolics analyses (A. Verma; K. Cherry, undergraduate student), and milling wheat samples (P. Lynn).

LITERATURE CITED

(1) Lin, W.; Vocke, G. Hard white wheat: changing the color of US wheat? Agricultural Outlook; Economic Research Service, USDA, Washington, DC, 1998; available online at www.ers.usda.gov/publications/agoutlook/aug1998/ao253e.pdf (verified Jan 2008).

(2) Miyamoto, T.; Everson, E. H. Biochemical and physiological studies of wheat grain pigmentation. *Agron. J.* **1958**, *50*, 733–734.

(3) Lepiniec, L.; Debeaujon, I.; Routaboul, J. M.; Nesi, N.; Caboche, M. Genetics and biochemistry of seed flavonoids. *Annu. Rev. Plant Biol.* **2006**, *57*, 405–430.

(4) Taiz, L.; Zeiger, E. In *Plant Physiology*, 3rd ed.; Sinauer Associates: Sunderland, MA, 2002; pp 290–297.

(5) Debeaujon, I.; Peters, A. J. M.; Leon-Kloosterziel, K. M.; Koornneef, M. The TRANSPARENT TESTA12 gene of *Arabidopsis* encodes a multidrug secondary transporter-like protein required for flavonoid sequestration in vacuoles of the seed coat endothelium. *Plant Cell.* **2001**, *13*, 853–871.

(6) Copper, D. C.; Sorrells, M. E. Selection for white kernel color in the progeny of red × white crosses. *Euphytica* **1984**, *33*, 227–232.

(7) Metzger, R. J.; Silbaugh, B. A. Location of genes for seed coat color in hexaploid wheat *Triticum aestivum* L. *Crop Sci.* **1970**, *10*, 495–496.

(8) McIntosh, R. A.; Yamazaki, Y.; Devos, K. M.; Dubcovsky, J.; Rogers, J.; Appels, R. Catalogue of gene symbols for wheat; 2003; available from www.shigen.nig.ac.jp/wheat/komugi/genes/download.jsp (verified Jan 2008).

(9) Baker, R. J. Inheritance of seed coat color in eight spring wheat cultivars. *Can. J. Plant Sci.* **1981**, *61*, 719–721.

(10) Himi, E.; Noda, K. Red grain color gene (*R*) of wheat is a Myb-type transcription factor. *Euphytica* **2005**, *143*, 239–242.

(11) Freed, R. D.; Everson, E. H.; Ringlund, K.; Gullord, M. Seed coat in wheat and the relationship to seed dormancy at maturity. *Cereal Res. Commun.* **1976**, *4*, 147–148.

(12) Reitan, L. Genetical aspects of seed dormancy in wheat related to seed coat color. *Cereal Res. Commun.* **1980**, *8*, 275–276.

(13) Lamkin, W. M.; Miller, B. S. Note on the uses of sodium hydroxide to distinguish red wheat from white common club and durum cultivars. *Cereal Chem.* **1980**, *57*, 293–294.

(14) Matus-Cádiz, M. A.; Hucl, P.; Perron, C. E.; Tyler, R. T. Genotype × environment interaction for grain color in hard white spring wheat. *Crop Sci.* **2003**, *43*, 219–226.

(15) Hucl, P.; Matus-Cadiz, M. A. W98616, a white-seeded spring wheat with increased pre-harvest sprouting resistance. *Can. J. Plant Sci.* **2002**, *82*, 129–131.

(16) Noll, J. S.; Dyck, P. L.; Czarnecki, E. Expression of RL4137 type dormancy in F1 seeds of reciprocal crosses in common wheat. *Can. J. Plant Sci.* **1982**, *62*, 345–349.

(17) Kaneko, S.; Komae, K.; Nagamine, T.; Yamada, T. Development of an extraction procedure for wheat red coat pigments and determination of varietal differences for this trait. *Breed. Sci.* **1994**, *44*, 263–266.

(18) Aharoni, A.; De Vos, R. C. H.; Verhoeven, H. A.; Maliepaard, C. A.; Kruppa, G.; Bino, R.; Goodenowe, D.B. Non-targeted metabolome analysis by use of fourier transform ion cyclotron mass spectrometry. *Omics* **2002**, *6*, 217–243.

(19) Hirai, M. Y.; Yano, M.; Goodenowe, D. B.; Kanaya, S.; Kimura, T.; Awazuhara, M.; Arita, M.; Fujiwara, T.; Saito, K. Integration of transcriptomics and metabolomics for understanding of global responses to nutritional stress in *Arabidopsis thaliana*. *Proc. Natl. Acad. Sci. U.S.A.* **2004**, *101*, 10205–10210.

(20) Debeaujon, I.; Léon-Kloosterziel, K. M.; Koornneef, M. Influence of the testa on seed dormancy germination, and longevity in *Arabidopsis*. *Plant Physiol.* **2000**, *122*, 403–413.

(21) Adom, K. K.; Sorrells, M. E.; Liu, R. H. Phytochemical profiles and antioxidant activity of wheat varieties. *J. Agric. Food Chem.* **2003**, *51*, 7825–7834.

(22) Krygier, K.; Sosulski, F.; Hogge, L. Free esterified, and insoluble-bound phenolic-acids.1. Extraction and purification procedure. *J. Agric. Food Chem.* **1982**, *30*, 330–334.

(23) Singleton, V. L.; Orthofer, R.; Lamuela-Raventós, R. M. Analysis of total phenols and other oxidation substrates and antioxidants by means of Folin−Ciocalteu reagent. *Methods Enzymol.* **1999**, *299*, 152–178.

(24) Daskalchuk, T. E.; Ahiahonu, P.; Heath, D.; Yamazaki, Y. In *Biotechnology in Agriculture and Forestry*; Saito, K., et al., Eds.; Springer: New York, 2006; pp 311–325.

(25) Pomeranz, Y. *Wheat Chemistry and Technology*, 3rd ed.; AACC: St. Paul, MN, 1998; pp 47−95.

(26) McCallum, J. A.; Walker, J. R. L. Proanthocyanidins in wheat bran. *Cereal Chem.* **1990**, *67*, 282–285.

(27) Pourcel, L.; Routaboul, J. M.; Cheynier, V.; Lepiniec, L.; Debeaujon, I. Flavonoid oxidation in plants: from biochemical properties to physiological functions. *Trends Plant Sci.* **2007**, *12*, 29–36, available at http://www.aseanbiotechnology.info/Abstract/21021117.pdf (verified Jan 2008).

(28) Marles, M. A.; Gruber, M. Y. Histochemical characterization of unextractable seed coat pigments and quantification of extractable lignin in the *Brassicaceae*. *J. Sci. Food Agric.* **2004**, *84*, 251–262.

(29) Himi, E.; Nisar, A.; Noda, K. Color genes (*R* and *Rc*) for grain and coleoptile upregulate flavonoid biosynthesis genes in wheat. *Genome* **2005**, *48*, 747–754.

(30) Himi, E.; Noda, K. Isolation and location of three homoeologous *dihydroflavonol-4-reductase* (DFR) genes of wheat and their tissue dependent expression. *J. Exp. Bot.* **2004**, *53*, 1569–1574.
(31) Stracke, R.; Ishihara, H.; Huep, G.; Barsch, A.; Mehrtens, F.; Niehaus, K.; Weisshaar, B. Differential regulation of closely related R2R3-MYB transcription factors controls flavonol accumulation in different parts of the *Arabidopsis thaliana* seedling. *Plant J.* **2007**, *50*, 660–677.
(32) Kristensen, H.; Aastrup, S. A non-destructive screening method for proanthocyanidin-free barley mutants. *Carlsberg Res. Commun.* **1986**, *51*, 509–513.
(33) Abdel-Aal, E. S. M.; Hucl, P. A rapid method for quantifying total anthocyanins in blue aleurone and purple pericarp wheats. *Cereal Chem.* **1999**, *76*, 350–354.

Received for review October 9, 2007. Revised manuscript received January 2, 2008. Accepted January 6, 2008. Financial support for this research was provided by grants from the SADF (Saskatchewan Agriculture Development Fund) and SAFRR (Saskatchewan Agriculture, Food and Rural Revitalization).

JF072970C